

## Structure and function of the platelet integrin $\alpha_{IIb}\beta_3$

Joel S. Bennett

*J Clin Invest.* 2005;115(12):3363-3369. <https://doi.org/10.1172/JCI26989>.

### Review Series

The platelet integrin  $\alpha_{IIb}\beta_3$  is required for platelet aggregation. Like other integrins,  $\alpha_{IIb}\beta_3$  resides on cell surfaces in an equilibrium between inactive and active conformations. Recent experiments suggest that the shift between these conformations involves a global reorganization of the  $\alpha_{IIb}\beta_3$  molecule and disruption of constraints imposed by the heteromeric association of the  $\alpha_{IIb}$  and  $\beta_3$  transmembrane and cytoplasmic domains. The biochemical, biophysical, and ultrastructural results that support this conclusion are discussed in this Review.

**Find the latest version:**

<https://jci.me/26989/pdf>





# Structure and function of the platelet integrin $\alpha_{IIb}\beta_3$

Joel S. Bennett

Hematology-Oncology Division, Department of Medicine, University of Pennsylvania School of Medicine, Philadelphia, Pennsylvania, USA.

**The platelet integrin  $\alpha_{IIb}\beta_3$  is required for platelet aggregation. Like other integrins,  $\alpha_{IIb}\beta_3$  resides on cell surfaces in an equilibrium between inactive and active conformations. Recent experiments suggest that the shift between these conformations involves a global reorganization of the  $\alpha_{IIb}\beta_3$  molecule and disruption of constraints imposed by the heteromeric association of the  $\alpha_{IIb}$  and  $\beta_3$  transmembrane and cytoplasmic domains. The biochemical, biophysical, and ultrastructural results that support this conclusion are discussed in this Review.**

Integrins are ubiquitous transmembrane  $\alpha/\beta$  heterodimers that mediate diverse processes requiring cell-matrix and cell-cell interactions such as tissue migration during embryogenesis, cellular adhesion, cancer metastases, and lymphocyte helper and killer cell functions (1). Eighteen integrin  $\alpha$  subunits and 8 integrin  $\beta$  subunits have been identified in mammals that combine to form 24 different heterodimers. The resulting heterodimers can then be grouped into subfamilies according to the identity of their  $\beta$  subunit (1). Platelets express 3 members of the  $\beta_1$  subfamily ( $\alpha_{IIb}\beta_1$ ,  $\alpha_v\beta_1$ , and  $\alpha_v\beta_1$ ) that support platelet adhesion to the ECM proteins collagen, fibronectin, and laminin, respectively (2–5), and both members of the  $\beta_3$  subfamily ( $\alpha_v\beta_3$  and  $\alpha_{IIb}\beta_3$ ). Although  $\alpha_v\beta_3$  mediates platelet adhesion to osteopontin and vitronectin in vitro (6, 7), it is uncertain whether it plays a role in platelet function in vivo. By contrast,  $\alpha_{IIb}\beta_3$ , a receptor for fibrinogen, vWF, fibronectin, and vitronectin, is absolutely required for platelet aggregation. Consequently, inherited abnormalities in  $\alpha_{IIb}\beta_3$  number or function preclude platelet aggregation, resulting in the bleeding disorder Glanzmann thrombasthenia (8). Conversely, thrombi that arise in the arterial circulation result from the  $\alpha_{IIb}\beta_3$ -mediated formation of platelet aggregates (9). Because  $\alpha_{IIb}\beta_3$  plays an indispensable role in hemostasis and thrombosis, it is among the most intensively studied integrins. Thus, there is a wealth of new information relating  $\alpha_{IIb}\beta_3$  structure and function, the subject of this Review.

Expression of  $\alpha_{IIb}\beta_3$  is restricted to cells of the megakaryocyte lineage. In megakaryocytes,  $\alpha_{IIb}\beta_3$  is assembled from  $\alpha_{IIb}$  and  $\beta_3$  precursors in the endoplasmic reticulum (10) and undergoes post-translational processing in the Golgi complex, where  $\alpha_{IIb}$  is cleaved into heavy and light chains (11). There are approximately 80,000 copies of  $\alpha_{IIb}\beta_3$  on the surface of unstimulated platelets (12), and additional heterodimers in the membranes of platelet granules are translocated to the platelet surface during platelet secretion (13). A critical feature of  $\alpha_{IIb}\beta_3$  function is that it is modulated by platelet agonists. Thus, while  $\alpha_{IIb}\beta_3$  can support the adhesion of unstimulated platelets to many of its ligands when they are immobilized in vitro, platelet stimulation is required to enable  $\alpha_{IIb}\beta_3$  to mediate platelet aggregation by binding soluble fibrinogen and vWF (14). EM images of rotary-shadowed  $\alpha_{IIb}\beta_3$  reveal that the heterodimer consists of an 8-by-12-nm nodular head containing its

ligand-binding site and two 18-nm flexible stalks containing its transmembrane (TM) and cytoplasmic domains (15).

## Crystal structures for the extracellular portions of $\alpha_v\beta_3$ and $\alpha_{IIb}\beta_3$

A major advance in understanding the structure and function of  $\alpha_{IIb}\beta_3$  resulted from the reports of crystal structures for the extracellular portions of  $\alpha_{IIb}\beta_3$  (16) and the closely related integrin  $\alpha_v\beta_3$  (17). Xiong and coworkers prepared crystals of a presumably activated conformation of the  $\alpha_v\beta_3$  extracellular region grown in the presence of  $Ca^{2+}$  (17). Surprisingly, the crystals revealed that the head region was severely bent over 2 nearly parallel tails (Figure 1). When the structure was extended, its appearance and dimensions were consistent with rotary-shadowed EM images of  $\alpha_{IIb}\beta_3$ . The structure itself revealed that the amino terminus of  $\alpha_v$  was folded into a  $\beta$ -propeller configuration, followed by a “thigh” and 2 “calf” domains, constituting the extracellular portion of the  $\alpha_v$  stalk. The  $\alpha_v$  “knee” or “genu,” the site at which the head region bends, was located between the thigh and first calf domain. The  $\beta_3$  head consists of a  $\beta A$  domain whose fold resembles that of integrin  $\alpha$  subunit “I-domains” and contains a metal ion-dependent adhesion site (MIDAS) motif, as well as a hybrid domain whose fold is similar to that of I-set Ig domains. The interface between the  $\alpha_v$   $\beta$ -propeller and the  $\beta_3$   $\beta A$  domain, the site at which the  $\alpha_v$  head interacts with the  $\beta_3$  head, resembles the interface between the  $G\alpha$  and  $G\beta$  subunits of G proteins. The  $\beta_3$  stalk consists of a PSI (plexin, semaphorin, integrin) domain, 4 tandem EGF repeats, and a unique carboxyterminal  $\beta TD$  domain. A cyclic Arg-Gly-Asp-containing (RGD-containing) pentapeptide, soaked into the crystal in the presence of  $Mn^{2+}$  (18), inserted into a crevice between the  $\beta$ -propeller and  $\beta A$  domains with the Arg side chain located in a groove on the upper surface of the propeller and the Asp carboxylate protruding into a cleft between loops on the  $\beta A$  surface, implying that the crevice constitutes at least a portion of the binding site for RGD-containing  $\alpha_v\beta_3$  ligands.

Subsequently, Xiao et al. reported 2 crystal structures of a complex consisting of the  $\alpha_{IIb}$   $\beta$ -propeller and the  $\beta_3$   $\beta A$ , hybrid, and PSI domains (16). The structures revealed an open, presumably high-affinity conformation, similar to EM images of the  $\alpha_v\beta_3$  extracellular domain-containing ligand, with a  $62^\circ$  angle of separation between the  $\alpha$  and  $\beta$  subunits due in part to a 10-Å downward movement of the  $\alpha_7$  helix of the  $\beta A$  domain relative to the hybrid and the PSI domain. Reorganization of hydrogen bonds in the interface between the  $\alpha_7$  helix and  $\beta C$  strand of the hybrid domain allowed the hybrid domain and the rigidly connected PSI domain to swing out, causing a 70-Å separation of the  $\alpha_{IIb}$  and  $\beta_3$  stalks at their “knees,” a feature noted in EM images of active forms of  $\alpha_{IIb}\beta_3$  in the presence or absence of ligand (19).

**Nonstandard abbreviations used:** GpA, glycoprotein A; MIDAS, metal ion-dependent adhesion site; PSI, plexin, semaphorin, integrin; RGD, Arg-Gly-Asp; TM, transmembrane.

**Conflict of interest:** The author has declared that no conflict of interest exists.

**Citation for this article:** *J. Clin. Invest.* 115:3363–3369 (2005). doi:10.1172/JCI26989.

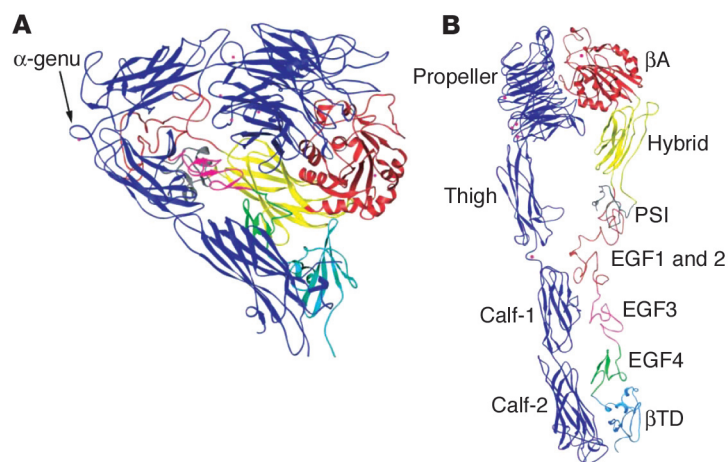


**Figure 1**

Ribbon diagram of the structure of the extracellular portion of  $\alpha_v\beta_3$ . (A) Bent conformation of  $\alpha_v\beta_3$  as it was present in the crystal. (B) Extension of the structure to reveal its domains. Adapted with permission from *Annual Review of Cell and Developmental Biology* (97).

### Ligand binding to $\alpha_{IIb}\beta_3$

Fibrinogen, the major  $\alpha_{IIb}\beta_3$  ligand, is composed of pairs of A $\alpha$ , B $\beta$ , and  $\gamma$  chains folded into 3 nodular domains. Although peptides corresponding to either the carboxyterminal 10–15 amino acids of the  $\gamma$  chain (20) or the 2  $\alpha$  chain RGD motifs inhibit fibrinogen binding to  $\alpha_{IIb}\beta_3$  (21), only the  $\gamma$  chain sequence is required for fibrinogen binding to  $\alpha_{IIb}\beta_3$  (22). Nonetheless, RGD-based peptides and peptidomimetics inhibit  $\alpha_{IIb}\beta_3$  function in vitro and are clinically effective antagonists of  $\alpha_{IIb}\beta_3$  function in vivo (23). The structural basis for these observations is not entirely clear, but competitive binding measurements indicate that  $\gamma$  chain and RGD peptides cannot bind to  $\alpha_{IIb}\beta_3$  at the same time (24), implying that RGD peptides inhibit fibrinogen binding by preventing the interaction of the  $\gamma$  chain with  $\alpha_{IIb}\beta_3$ .

Ligand binding to  $\alpha_{IIb}\beta_3$  involves specific regions of the amino-terminal portions of both  $\alpha_{IIb}$  and  $\beta_3$ . In the crystal structure of the  $\alpha_{IIb}\beta_3$  head domain, ligand binds to a “specificity-determining” loop in the  $\beta_3$   $\beta$ A domain and to a “cap” composed of 4 loops on the upper surface of the  $\alpha_{IIb}$   $\beta$ -propeller domain (16). The  $\alpha_{IIb}$   $\beta$ -propeller results from the folding of 7 contiguous aminoterminal repeats (17, 25). Each blade of the propeller is formed from 4 antiparallel  $\beta$  strands located in each repeat; loops connecting the strands are located on either the upper or the lower surface of the propeller. A number of naturally occurring and laboratory-induced mutations distributed between  $\alpha_{IIb}$  residues 145 and 224 and located in loops on the upper surface of the propeller impair  $\alpha_{IIb}\beta_3$  function, implying that these residues interact with ligand (26–28). Further, Kamata et al. replaced each of the 27 loops in the  $\alpha_{IIb}$  propeller with the corresponding loops from  $\alpha_4$  or  $\alpha_5$  (29). They found that 8 replacements, all located on the upper surface of the second, third, and fourth repeats, abrogated fibrinogen binding to  $\alpha_{IIb}\beta_3$ , suggesting that fibrinogen binds to the upper surface of the propeller in a region centered around the third repeat. Previous chemical cross-linking experiments suggested that the fibrinogen  $\gamma$  chain binds to  $\alpha_{IIb}$  in the vicinity of its second calmodulin-like motif near amino acids 294–314 (30), but these residues are located on the lower surface of the propeller and are unlikely to interact with ligands such as fibrinogen (16). It is noteworthy that ligand binding itself induces conformational changes in  $\alpha_{IIb}\beta_3$ , most often detected by the appearance of neoepitopes for mAbs. In fact, such ligand-induced changes or LIBSs (ligand-induced binding sites) may be responsible for the

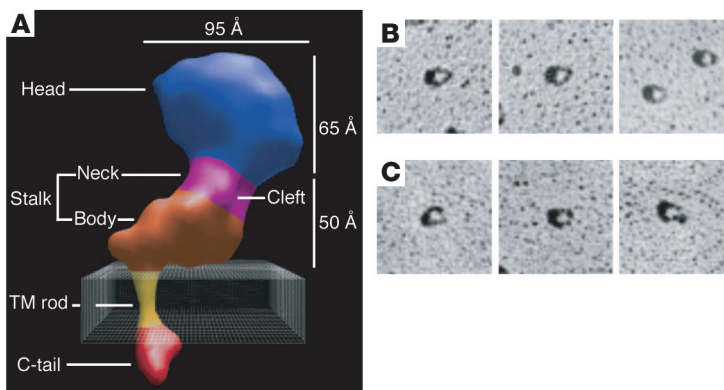
immune-mediated thrombocytopenia associated with the clinical use of  $\alpha_{IIb}\beta_3$  antagonists (31).

Ligand binding to  $\alpha_{IIb}\beta_3$  requires divalent cations (32). Eight divalent cation-binding sites were identified in the  $\alpha_v\beta_3$  crystal structure (17, 18). Four were located in the  $\alpha_v$   $\beta$ -propeller domain, 1 at the  $\alpha_v$  genu, and 3 in the  $\beta_3$   $\beta$ A domain, but only those located in the  $\beta$ A domain appeared to participate in ligand binding. In the absence of ligand, only the  $\beta$ A ADMIDAS (adjacent to the metal ion-dependent adhesion site) motif was occupied, but when  $Mn^{2+}$  and a cyclic RGD ligand were present, each of the  $\beta$ A sites contained a cation. One site was the  $\beta$ A MIDAS;  $Mn^{2+}$  present at this site was in direct contact with ligand. A second  $Mn^{2+}$ , located 6 Å from the MIDAS, was bound to a site designated ligand-induced metal-binding site (LIMBS), but the cation at this site did not interact with ligand. It had been postulated that  $Mn^{2+}$  induces integrin activation by antagonizing inhibitory effects of  $Ca^{2+}$  (33), but the  $\alpha_v\beta_3$  crystal structure suggests that cations bound to the MIDAS and LIMBS motifs act by stabilizing the ligand-occupied conformation of the  $\beta$ A domain (18).

### Regulation of $\alpha_{IIb}\beta_3$ ligand-binding activity

Integrins reside on cell surfaces in an equilibrium between inactive and active conformations (34). In experiments where the cytoplasmic domains of  $\alpha_L\beta_2$  and  $\alpha_5\beta_1$  were replaced by acidic and basic peptides (35, 36), purified integrins were inactive when their stalks were in proximity and active when the stalks were farther apart. This was corroborated by measurements of fluorescence resonance energy transfer (FRET) efficiency between cyan and yellow fluorescent proteins fused to the cytoplasmic domains of  $\alpha_L$  and  $\beta_2$  expressed in K562 cells (37). FRET efficiency decreased when  $\alpha_L\beta_2$  interacted with immobilized or soluble ligand, implying that bidirectional signaling resulted from the coupling of conformational changes in the  $\alpha_L\beta_2$  extracellular domain to the spatial separation of the  $\alpha_L$  and  $\beta_2$  cytoplasmic domains, a result consistent with EM images of  $\alpha_{IIb}\beta_3$  in which scissor-like movements of the  $\alpha_{IIb}$  and  $\beta_3$  stalks differentiate active and inactive molecules (19).

Nonetheless, the relationship of these observations to the  $\alpha_{IIb}\beta_3$  and  $\alpha_v\beta_3$  crystal structures is controversial. Takagi et al., supported by negatively stained EM images of active and inactive integrins, suggested that the bent conformation of  $\alpha_v\beta_3$  in crystals corresponds to low-affinity  $\alpha_v\beta_3$  and the shift to a high-affinity conformation occurs when the integrin undergoes a global reorganization characterized by a “switchblade-like” opening to an extended structure and scissor-like separation of the  $\alpha$  and  $\beta$  subunit stalks (34). Xiong et al., however, suggested that the bent conformation resulted from flexibility at the  $\alpha_v$  and  $\beta_3$  genua and from crystal contacts not likely to occur in nature (17). This possibility was supported by cryo-EM reconstructions of intact inactive  $\alpha_{IIb}\beta_3$  molecules, which revealed a collapsed but unbent structure consisting of a large globular head and an L-shaped stalk whose axis was rotated approximately 60° with respect to the head and was

**Figure 2**

Cryo-EM reconstruction and rotary-shadowed EM images of  $\alpha_{IIB}\beta_3$ . **(A)** Cryo-EM reconstruction. The resolution is 20 Å. Adapted with permission from *Proceedings of the National Academy of Sciences of the United States of America* (38). **(B and C)** Rotary-shadowed EM images. The images in **B** were obtained in the presence of 1 mM  $\text{Ca}^{2+}$  and the images in **C** in the presence of 1 mM  $\text{Mn}^{2+}$ . Reproduced with permission from *Blood* (19).

connected at an angle of approximately  $90^\circ$  to a rod containing the TM domains of the integrin (Figure 2A) (38). They also suggested that extension at the “knees” may be a post-ligand-binding “outside-in” signaling event and that the transition of  $\alpha\beta_3$  from its inactive to its active conformation results when the CD loop of the  $\beta_3$   $\beta$ TD domain moves away from the  $\beta$ A domain, allowing the latter to assume its active conformation (39). How to reconcile each of these models with the rotary-shadowed EM images of demonstrably inactive and active  $\alpha_{IIB}\beta_3$  shown in Figure 2, B and C, is not obvious.

### The $\alpha_{IIB}$ and $\beta_3$ cytoplasmic domains constrain $\alpha_{IIB}\beta_3$ function

Cytoplasmic domain sequences, most convincingly demonstrated for conserved membrane-proximal sequences, constrain integrins in their low-affinity (inactive) conformations. Thus, truncation of the  $\alpha_{IIB}$  cytoplasmic domain at Gly991 or the  $\beta_3$  cytoplasmic domain at Leu717 or deletion of the conserved membrane-proximal  $\alpha_{IIB}$  GFFKR or  $\beta_3$  LLTIHD motifs (Table 1) shifts  $\alpha_{IIB}\beta_3$  to its active state (40). Similarly, constitutive  $\alpha_{IIB}\beta_3$  function can be induced by replacement of  $\alpha_{IIB}$  residue F992, F993, or R995 or  $\beta_3$  residue D723 with alanine, whereas heterodimers containing simultaneous R995→D and D723→R substitutions are inactive (41). These observations led to the suggestion that the membrane-proximal sequences form an activation-constraining “clasp,” an essential feature of which is a salt bridge between  $\alpha_{IIB}$  R995 and  $\beta_3$  D723. Paradoxically, replacing the  $\alpha_{IIB}$  cytoplasmic domain with the cytoplasmic domain of  $\alpha_2$ ,  $\alpha_5$ ,  $\alpha_{6A}$ , or  $\alpha_{6B}$ , each of which contains a GFFKR motif, activates  $\alpha_{IIB}\beta_3$  (40). This implies that additional cytoplasmic domain sequences modulate  $\alpha_{IIB}\beta_3$  function, consistent with the inhibitory effects observed for the  $\beta_3$  mutation Ser752Pro (42),  $\beta_3$  truncation at Arg724 (43), and mutations involving the  $\beta_3$  sequences EFAKFEEE, NPLY, and NITY (44–46) and the  $\alpha_{IIB}$  sequence Pro998/Pro999 (47, 48).

Interaction between the  $\alpha_{IIB}$  and  $\beta_3$  cytoplasmic domains has been studied experimentally using peptides dissolved in aqueous buffer or anchored to phospholipid micelles via aminoterminal myristoylation. Using terbium luminescence and electrospray ionization mass spectroscopy, Haas and Plow observed the formation of a cation-containing complex involving  $\alpha_{IIB}$  residues 999–1,008 and  $\beta_3$  residues 721–740 (49). Similarly, Vallar et al. used surface plasmon resonance to detect a weak ( $K_d \sim 50 \mu\text{M}$ ) KVGFFKR-dependent, calcium-stabilized

complex between soluble  $\alpha_{IIB}$  cytoplasmic domain and immobilized  $\beta_3$  cytoplasmic domain peptides (50). Further, Weljie et al. determined an NMR structure for a heterodimer that formed at low ionic strength between an 11-residue GFFKR-containing  $\alpha_{IIB}$  peptide and a 25-residue LLTIHD-containing  $\beta_3$  peptide (51). They identified 2 conformers differing in the conformation of the  $\beta_3$  backbone: one had an elongated  $\beta_3$  structure; the other was bent back at D723–A728, causing the peptide to adopt a closed L shape. Nonetheless, both conformers were predominantly helical with significant hydrophobic interactions between V990 and F993 of  $\alpha_{IIB}$  and L717–I721 of  $\beta_3$ . Although there was no NMR evidence of an R995–D723 salt bridge, modeling suggested that a salt bridge was possible if the  $\beta_3$  backbone was elongated. Vinogradova et al. also used NMR to characterize complexes between full-length  $\alpha_{IIB}\beta_3$  cytoplasmic domain peptides (48, 52, 53). Despite low affinity, they identified interfaces for the complexes that included hydrophobic and electrostatic interactions between membrane-proximal helices (Figure 3A) (52). When the experiments were repeated in the presence of diphosphocholine micelles,  $\alpha_{IIB}$  residues 989–993 and  $\beta_3$  residues 716–721 were embedded in lipid and there was interaction between  $\beta_3$  residues 741 and 747 and micelle lipid (53). Talin binding to  $\beta_3$  disrupted the complex of  $\alpha_{IIB}$  with  $\beta_3$  as well as  $\beta_3$  interaction with lipid (Figure 3B). On the other hand, Li et al. were unable to detect heteromeric interaction between proteins corresponding to the  $\alpha_{IIB}$  and  $\beta_3$  TM and cytoplasmic domains in diphosphocholine micelles at physiologic salt concentrations using a number of biophysical techniques, perhaps because heteromeric interaction is substantially weaker than homomeric interaction (54). Similarly, Ulmer et al. did not detect heteromeric

**Table 1**

Amino acid sequences of the TM and cytoplasmic domains of  $\alpha_{IIB}$  and  $\beta_3^A$

#### TM domains

$\alpha_{IIB}$	W <sub>968</sub> VLVGVLGGLLLLTILVLMW <sub>988</sub>
$\beta_3$	I <sub>693</sub> LVVLLSVMGAILLIGLAALLIW <sub>715</sub>

#### Cytoplasmic domains

$\alpha_{IIB}$	K <sub>989</sub> VGFFKRNRPPLLEEDDEEGE <sub>1008</sub>
$\beta_3$	K <sub>716</sub> LLTIHDRKEFAKFEERARAKWDANNPLYKEATSTFTNITYRGT <sub>762</sub>

<sup>A</sup>The amino acids in the  $\alpha_{IIB}$  and  $\beta_3$  TM and cytoplasmic domains are designated in the single-letter code; the subscript numbers correspond to the position of the preceding amino acid in the sequence for mature  $\alpha_{IIB}$  and  $\beta_3$  (98, 99). The  $\alpha_{IIB}$  GxxxG motif,  $\beta_3$  G708, the membrane-proximal regions of both cytoplasmic domains, and both  $\beta_3$  NxxY motifs are underlined.

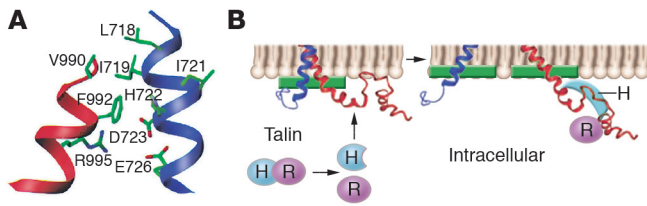


**Figure 3**  
Interaction of the  $\alpha_{IIb}$  and  $\beta_3$  cytoplasmic domains. **(A)** Backbone ribbon diagram of the  $\alpha_{IIb}\beta_3$  membrane-proximal cytoplasmic domain clasp showing hydrophobic and electrostatic interactions. Reproduced with permission from *Cell* (52). **(B)** Model of the changes that may occur in the clasp following talin binding to the  $\beta_3$  cytoplasmic domain. Adapted with permission from *Proceedings of the National Academy of Sciences of the United States of America* (53).

interactions of  $\alpha_{IIb}$  with  $\beta_3$  in an NMR analysis of a coiled-coil construct containing the  $\alpha_{IIb}$  and  $\beta_3$  cytoplasmic domains (55).

**Proteins that interact with the  $\alpha_{IIb}$  and  $\beta_3$  cytoplasmic domains**

Proteins have been identified, most often using yeast 2-hybrid screens, that bind to the cytoplasmic domains of integrin  $\alpha$  and  $\beta$  subunits. These proteins include CIB (calcium- and integrin-binding protein) (56), Aup1 (ancient ubiquitous protein 1) (57), ICLn (a chloride channel regulatory protein) (58), and PP1c (the catalytic subunit of protein phosphatase 1) (59), each of which binds to the membrane-proximal  $\alpha_{IIb}$  sequence KVGFFKR. However, because a substantial portion of this sequence is likely embedded in the plasma membrane (60, 61), the physiologic importance of these interactions is uncertain. Proteins that interact with the  $\beta_3$  cytoplasmic domain include the cytoskeletal proteins talin,  $\alpha$ -actinin, filamin, myosin, and skelemin; various members of the Src family of kinases; the kinases integrin-linked kinase (ILK), Syk, and Shc; the adaptor Grb2; the scaffold RACK1; CD98 (62); and  $\beta_3$ -endoneixin (63). Binding of myosin, Shc, and Grb2 requires platelet aggregation and spreading, as well as the Fyn-mediated phosphorylation of  $\beta_3$  tyrosines 747 and 759, and has been implicated in post-receptor-binding cytoskeleton-mediated events such as clot retraction (64).

Binding of  $\beta_3$ -endoneixin or talin to the  $\beta_3$  cytoplasmic domain is noteworthy because it can activate  $\alpha_{IIb}\beta_3$ .  $\beta_3$ -Endoneixin, a 14-kDa protein of unknown function, induces  $\alpha_{IIb}\beta_3$  activation when coexpressed with  $\alpha_{IIb}\beta_3$  in tissue culture cells by interacting with residues located in both the aminoterminal and the carboxyterminal regions of the  $\beta_3$  cytoplasmic domain, in particular the carboxyterminal NITY motif (65–67). Nonetheless, there is no evidence as yet that  $\beta_3$ -endoneixin regulates  $\alpha_{IIb}\beta_3$  function in platelets. One explanation for the presence of 2 discontinuous  $\beta_3$ -endoneixin-binding sites in the  $\beta_3$  cytoplasmic domain has been provided by an NMR analysis of a protein encompassing the  $\beta_3$  TM and cytoplasmic domains (Figure 4) (68). This analysis revealed that the  $\beta_3$  TM helix extended into the membrane-proximal region of the cytoplasmic domain, ending at an apparent hinge at residues H722–D723 (Table 1). Two additional helical stretches, extending from residues 725 to 735 and 748 to 755, were also present (Figure 4). Because the latter helices can interact with each other, they can place the proximal and distal regions of the  $\beta_3$  cytoplasmic domain in proximity.

Talin, an abundant 250-kDa cytoskeletal protein, forms antiparallel homodimers that bind to the cytoplasmic domain of integrin

$\beta$  subunits as well as to other cytoskeletal proteins such as actin and vinculin (69). Talin is composed of a 50-kDa head domain containing its principal integrin-binding site and a 220-kDa rod domain that binds to integrins with lesser affinity (69). The talin head itself contains an approximately 300-residue FERM (four-point-one, ezrin, radixin, moesin) domain that folds into F1, F2, and F3 subdomains (69). F2 and F3 bind to the  $\beta_3$  cytoplasmic domain, although the affinity of F3 binding is substantially greater (70). A crystal structure for a fusion protein composed of the F2 and F3 subdomains and a contiguous aminoterminal peptide corresponding to the midportion of the  $\beta_3$  cytoplasmic domain, including its NPLY motif, revealed that the interaction of the  $\beta_3$  peptide with F3 was mainly hydrophobic and that NPLY interacted with F3 in a manner that resembled that of canonical PTB domain ligands (71). However, studies using NMR also revealed that F3 and F2-F3 interact with the membrane-proximal region of the  $\beta_3$  cytoplasmic domain (71, 72), consistent with previous observations that talin binds to peptides corresponding to this portion of  $\beta_3$  (73).

Overexpressing the talin head domain in  $\alpha_{IIb}\beta_3$ -expressing CHO cells induces  $\alpha_{IIb}\beta_3$  activation (74), either directly because talin disrupts the clasp between  $\alpha_{IIb}$  and  $\beta_3$  (Figure 3B) or indirectly via conformational changes induced by F3 binding to the  $\beta_3$  NPLY motif (70). Conversely, reducing talin expression using short hairpin RNAs decreases ligand binding to  $\alpha_{IIb}\beta_3$  in CHO cells and in ES cell-derived agonist-stimulated megakaryocytes (75). Taken together, these results imply that talin binding to the  $\beta_3$  cytoplasmic domain may be a final step in  $\alpha_{IIb}\beta_3$  activation. Nonetheless, how talin binding to the  $\beta_3$  cytoplasmic domain is regulated remains to be determined. The integrin-binding domain in intact talin appears to be masked (76). Although the enzyme calpain can cleave talin, releasing its head domain (77), calpain activation in platelets is a relatively late step after platelet stimulation (78) and would be unlikely to contribute to integrin-activating inside-out signaling. On the other hand, talin binds to membrane-associated phosphoinositol 4,5-bisphosphate, inducing a conformational change that enables it to bind to the  $\beta_1$  cytoplasmic domain (79). By analogy, talin binding to phosphoinositol 4,5-bisphosphate may enable it to bind to  $\beta_3$ .

**Regulation of  $\alpha_{IIb}\beta_3$  function by TM domain interaction**

TM domain-mediated protein oligomerization is a common mechanism for the assembly of membrane proteins and regula-

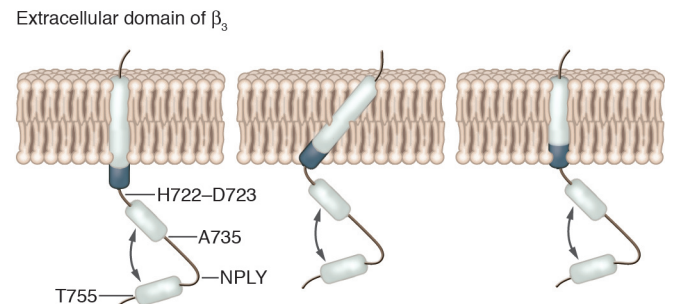


**Figure 4**  
Model of the structure of the  $\beta_3$  TM and cytoplasmic domains. Helices are shown as cylinders. Three different orientations of the  $\beta_3$  TM domain in the plasma membrane are shown. The membrane-proximal region of the cytoplasmic domain is shaded. Arrows indicate possible interactions between helices. Adapted with permission from *Biochemistry* (68).

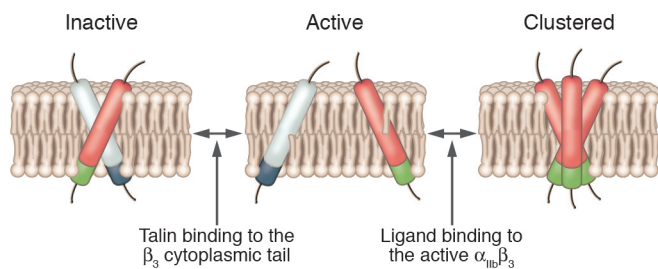
**Figure 5**

Diagram illustrating the “push-pull” hypothesis for regulation of the  $\alpha_{IIb}\beta_3$  activation state. The white and blue cylinders represent the  $\alpha_{IIb}$  TM and membrane-proximal cytoplasmic domain helices, respectively. The red and green cylinders represent the  $\beta_3$  TM and membrane-proximal cytoplasmic domain helices, respectively.

tion of protein function (80). Specificity is achieved via specific sequence motifs superimposed on more general oligomerization frameworks (81–83). For example, the sequence motif GxxxG, first recognized as a framework for the homomeric association of the glycophorin A (GpA) TM helix (81), has been identified as the most overrepresented sequence motif in TM domain databases (82).

With regard to integrin TM domains, Li and coworkers reported that peptides corresponding to the  $\alpha_{IIb}$  and  $\beta_3$  TM domains readily undergo homodimeric and homotrimeric association, respectively, in phospholipid micelles (54), and Schneider and Engelman found that fusion proteins containing the  $\alpha_2\beta_1$ ,  $\alpha_4\beta_7$ , and  $\alpha_{IIb}\beta_3$  TM domains undergo integrin-specific TM domain-mediated homomeric and heteromeric association in bacterial membranes (84). Subsequently, Li et al. reported that facilitating the homomeric association of the  $\beta_3$  TM helix by replacing either G708 or M701 with a polar asparagine induced  $\alpha_{IIb}\beta_3$  activation and clustering when the mutants were expressed in CHO cells (85). They also found that mutation of the  $\alpha_{IIb}$  GxxxG motif located at residues 972–975 disrupted the homomeric association of  $\alpha_{IIb}$  TM helix (86) and paradoxically induced  $\alpha_{IIb}\beta_3$  activation and clustering (87). These observations suggested the “push-pull” mechanism for  $\alpha_{IIb}\beta_3$  activation shown in Figure 5. Processes that destabilize the association of the  $\alpha_{IIb}$  and  $\beta_3$  TM helices, such as talin binding to the  $\beta_3$  cytoplasmic domain, would be expected to promote dissociation of the helices with concomitant  $\alpha_{IIb}\beta_3$  activation. Conversely, intermolecular interactions that either require separation of the  $\alpha_{IIb}$  and  $\beta_3$  TM helices, such as homooligomerization, or are more favorable when they separate, such as ligand-induced  $\alpha_{IIb}\beta_3$  clustering (88), would be expected to pull the equilibrium toward the activated state.

The ability of homomeric TM helix interactions to induce  $\alpha_{IIb}\beta_3$  activation and clustering remains controversial (89, 90), but there is compelling evidence that heterodimeric interactions constrain  $\alpha_{IIb}\beta_3$  in a low-affinity state. By simultaneously scanning the  $\alpha_{IIb}$  and  $\beta_3$  TM helices with cysteine residues, Luo et al. detected the formation of disulfide bonds with a helical periodicity in a region corresponding to  $\alpha_{IIb}$  residues 966–974 and  $\beta_3$  residues 693–702, consistent with the presence of a unique  $\alpha_{IIb}\beta_3$  TM heterodimer (91). They also scanned the  $\alpha_{IIb}$  and  $\beta_3$  helices with leucines, confirming that mutation of the  $\alpha_{IIb}$  GxxxG motif induces  $\alpha_{IIb}\beta_3$  activation (90). Partridge et al. used random mutagenesis of the  $\beta_3$  TM and cytoplasmic domains to search for interactions constraining  $\alpha_{IIb}\beta_3$  activation (92). They detected 12 activating mutations in the mem-

brane-proximal cytoplasmic domain and 13 activating mutations in the  $\beta_3$  TM helix. Nine of the latter were predicted to shorten the helix, perhaps activating  $\alpha_{IIb}\beta_3$  by altering the tilt of the helix in the membrane (Figure 4). The remaining mutations were located in the carboxyterminal half of the helix and were postulated to activate  $\alpha_{IIb}\beta_3$  by disrupting the packing of an  $\alpha_{IIb}\beta_3$  TM heterodimer.

Despite the biochemical evidence supporting the presence of  $\alpha_{IIb}$  and  $\beta_3$  TM domain oligomers, their existence has not been confirmed by NMR spectroscopy or x-ray crystallography because of difficulty in obtaining high-resolution structures for TM proteins using these techniques. However, computational methods have been used to construct TM domain models incorporating the constraints imposed by mutational data. Based on cryo-EM images (Figure 2A), Adair and Yeager proposed that the TM domains of inactive  $\alpha_{IIb}\beta_3$  associate in a parallel  $\alpha$ -helical coiled coil (38). Using the R995–D723 salt bridge as the primary constraint, they found that a right-handed coiled coil based on the GpA TM dimer (93) placed more conserved residues in the helix-helix interface than a coiled coil based on the canonical left-handed leucine zipper. Gottschalk and coworkers proposed that the  $\alpha_{IIb}$  and  $\beta_3$  TM helices remain in close contact in the activated state and that the helix-helix interface is a GpA-like structure containing the  $\alpha_{IIb}$  G972xxxG975 and  $\beta_3$  S699xxxA703 motifs (94). Moreover, simulated annealing and molecular dynamics supported a model in which the  $\alpha_{IIb}$  and  $\beta_3$  TM domains interact weakly in a right-handed coiled coil when the integrin is in its low-affinity conformation (95). Subsequently, in order to account for both aminoterminal and carboxyterminal restraints, Gottschalk proposed that the  $\alpha_{IIb}\beta_3$  TM and membrane-proximal cytoplasmic domains form a right-handed coiled coil in which the helices interact over their entire length, placing the  $\alpha_{IIb}$  GxxxG motif, but not  $\beta_3$  S699xxxA703, in the helix-helix interface (96). By contrast, Luo et al. used their disulfide cross-linking data to construct a model based on the GpA TM dimer; however, in this model, the  $\alpha_{IIb}$  GxxxG-like motif corresponded to residues 968–972, rather than 972–975 (91). DeGrado and coworkers used a Monte Carlo-simulated annealing algorithm to obtain atomic models for an  $\alpha_{IIb}$  TM homodimer (86) and an  $\alpha_{IIb}\beta_3$  heterodimer (87). In each case, a family of structures was found that satisfied mutational constraints. For the  $\alpha_{IIb}$  homodimer, all structures had right-handed crossing angles ranging from 40° to 60°, but with an interface rotated by 50° relative to the GpA homodimer. In the case of the  $\alpha_{IIb}\beta_3$  heterodimer, initial docking identified local minima with both right- and left-handed crossing angles. However, the right-handed structures had lower energies and more extensive interactions, and the  $\alpha_{IIb}$  GxxxG motif was in intimate contact with the  $\beta_3$  TM domain. Lastly, Partridge et al., using a Monte Carlo simulation, obtained 2 structures for an  $\alpha_{IIb}\beta_3$  TM heterodimer with helix packing near either the amino or the carboxyl termini of the helices, respectively; of the 2 models, carboxyterminal helix packing was more consistent with their mutational data (92). It is obvious that there is wide disparity among these models, making it clear that obtaining actual structures for  $\alpha_{IIb}$  and  $\beta_3$  TM domain hetero- and homo-oligomers will be the next major advance in our understanding of the structural basis for the regulation of platelet integrin function.

Address correspondence to: Joel S. Bennett, Hematology-Oncology Division, Department of Medicine, University of Pennsylvania School of Medicine, 914 BRB II/III, 421 Curie Boulevard, Philadelphia, Pennsylvania 19104-6058, USA. Phone: (215) 573-3280; Fax: (215) 573-7039; E-mail: bennetts@mail.med.upenn.edu.



- Hynes, R.O. 2002. Integrins: bidirectional, allosteric signaling machines. *Cell*. **110**:673–687.
- Piotrowicz, R.S., Orzechowski, R.P., Nugent, D.J., Yamada, K.Y., and Kunicki, T.J. 1988. Glycoprotein Ic-IIa functions as an activation-independent fibronectin receptor on human platelets. *J. Cell Biol.* **106**:1359–1364.
- Ill, C.R., Engvall, E., and Ruoslahti, E. 1984. Adhesion of platelets to laminin in the absence of activation. *J. Cell Biol.* **99**:2140–2145.
- Sonnenberg, A., Modderman, P., and Hogervorst, F. 1988. Laminin receptor on platelets is the integrin VLA-6. *Nature*. **336**:487–488.
- Staatz, W.D., Rajpara, S.M., Wayner, E.A., Carter, W.G., and Santoro, S.A. 1989. The membrane glycoprotein Ia-IIa (VLA-2) complex mediates the Mg<sup>2+</sup>-dependent adhesion of platelets to collagen. *J. Cell Biol.* **108**:1917–1924.
- Bennett, J.S., Chan, C., Vilaire, G., Mousa, S.A., and DeGrado, W.F. 1997. Agonist-activated  $\alpha\beta_3$  on platelets and lymphocytes binds to the matrix protein osteopontin. *J. Biol. Chem.* **272**:8137–8140.
- Paul, B.Z.S., Vilaire, G., Kunapuli, S.P., and Bennett, J.S. 2003. Concurrent signaling from G $\alpha_q$ - and G $\alpha_i$ -coupled pathways is essential for agonist-induced  $\alpha\beta_3$  activation on human platelets. *J. Thromb. Haemost.* **1**:814–820.
- George, J.N., Caen, J.P., and Nurden, A.T. 1990. Glanzmann's thrombasthenia: the spectrum of clinical disease. *Blood*. **75**:1383–1395.
- Lefkovits, J., Plow, E., and Topol, E. 1995. Platelet glycoprotein IIb/IIIa receptors in cardiovascular medicine. *N. Engl. J. Med.* **332**:1553–1559.
- Duperray, A., et al. 1987. Biosynthesis and processing of platelet GPIIb-IIIa in human megakaryocytes. *J. Cell Biol.* **104**:1665–1673.
- Kolodziej, M.A., Vilaire, G., Gonder, D., Poncz, M., and Bennett, J.S. 1991. Study of the endoproteolytic cleavage of platelet glycoprotein IIb using oligonucleotide-mediated mutagenesis. *J. Biol. Chem.* **266**:23499–23504.
- Wagner, C.L., et al. 1996. Analysis of GPIIb/IIIa receptor number by quantitation of 7E3 binding to human platelets. *Blood*. **88**:907–914.
- Niija, K., et al. 1987. Increased surface expression of the membrane glycoprotein IIb/IIIa complex induced by platelet activation. Relationship to the binding of fibrinogen and platelet aggregation. *Blood*. **70**:475–483.
- Bennett, J.S. 1996. Structural biology of glycoprotein IIb-IIIa. *Trends Cardiovasc. Med.* **6**:31–37.
- Weisel, J.W., Nagaswami, C., Vilaire, G., and Bennett, J.S. 1992. Examination of the platelet membrane glycoprotein IIb/IIIa complex and its interaction with fibrinogen and other ligands by electron microscopy. *J. Biol. Chem.* **267**:16637–16643.
- Xiao, T., Takagi, J., Coller, B.S., Wang, J.H., and Springer, T.A. 2004. Structural basis for allostery in integrins and binding to fibrinogen-mimetic therapeutics. *Nature*. **432**:59–67.
- Xiong, J.P., et al. 2001. Crystal structure of the extracellular segment of integrin  $\alpha_V\beta_3$ . *Science*. **294**:339–345.
- Xiong, J.P., et al. 2002. Crystal structure of the extracellular segment of integrin  $\alpha_V\beta_3$  in complex with an Arg-Gly-Asp ligand. *Science*. **296**:151–155.
- Litvinov, R.I., et al. 2004. Functional and structural correlations of individual  $\alpha_{IIb}\beta_3$  molecules. *Blood*. **104**:3979–3985.
- Kloczewiak, M., Timmons, S., Lukas, T.J., and Hawiger, J. 1984. Platelet receptor recognition site on human fibrinogen. Synthesis and structure-function relationships of peptides corresponding to the carboxy-terminal segment of the  $\gamma$  chain. *Biochemistry*. **23**:1767–1774.
- Gartner, T.K., and Bennett, J.S. 1985. The tetrapeptide analogue of the cell attachment site of fibronectin inhibits platelet aggregation and fibrinogen binding to activated platelets. *J. Biol. Chem.* **260**:11891–11894.
- Farrell, D.H., Thiagarajan, P., Chung, D.W., and Davie, E.W. 1992. Role of fibrinogen  $\alpha$  and  $\gamma$  chain sites in platelet aggregation. *Proc. Natl. Acad. Sci. U. S. A.* **89**:10729–10732.
- Bennett, J.S. 2001. Novel platelet inhibitors. *Annu. Rev. Med.* **52**:161–184.
- Bennett, J.S., Shattil, S.J., Power, J.W., and Gartner, T.K. 1988. Interaction of fibrinogen with its platelet receptor. Differential effects of  $\alpha$  and  $\gamma$  chain fibrinogen peptides on the glycoprotein IIb-IIIa complex. *J. Biol. Chem.* **263**:12948–12953.
- Springer, T.A. 1997. Folding of the N-terminal, ligand-binding region of integrin  $\alpha$ -subunits into a  $\beta$ -propeller domain. *Proc. Natl. Acad. Sci. U. S. A.* **94**:65–72.
- Kamata, T., Irie, A., Tokuhira, M., and Takada, Y. 1996. Critical residues of integrin  $\alpha_{IIb}\beta_3$  subunit for binding of  $\alpha_{IIb}\beta_3$  (glycoprotein IIb-IIIa) to fibrinogen and ligand-mimetic antibodies (PAC-1, OP-G2, and LJ-CP3). *J. Biol. Chem.* **271**:18610–18615.
- Tozer, E.C., Baker, E.K., Ginsberg, M.H., and Loftus, J.C. 1999. A mutation in the  $\alpha$  subunit of the platelet integrin  $\alpha_{IIb}\beta_3$  identifies a novel region important for ligand binding. *Blood*. **93**:918–924.
- Basani, R.B., et al. 2000. A naturally occurring mutation near the amino terminus of  $\alpha_{IIb}$  defines a new region involved in ligand binding to  $\alpha_{IIb}\beta_3$ . *Blood*. **95**:180–188.
- Kamata, T., Tieu, K.K., Irie, A., Springer, T.A., and Takada, Y. 2001. Amino acid residues in the  $\alpha_{IIb}$  subunit that are critical for ligand binding to integrin  $\alpha_{IIb}\beta_3$  are clustered in the  $\beta$ -propeller model. *J. Biol. Chem.* **276**:44275–44283.
- D'Souza, S.E., Ginsberg, M.H., Burke, T.A., and Plow, E.F. 1990. The ligand binding site of the platelet integrin receptor GPIIb-IIIa is proximal to the second calcium binding domain of its  $\alpha$  subunit. *J. Biol. Chem.* **265**:3440–3446.
- Bougie, D.W., et al. 2002. Acute thrombocytopenia after treatment with tirofiban or eptifibatid is associated with antibodies specific for ligand-occupied GPIIb/IIIa. *Blood*. **100**:2071–2076.
- Bennett, J.S., and Vilaire, G. 1979. Exposure of platelet fibrinogen receptors by ADP and epinephrine. *J. Clin. Invest.* **64**:1393–1401.
- Smith, J., Piotrowicz, R., and Mathis, D. 1994. A mechanism for divalent cation regulation of beta 3-integrins. *J. Biol. Chem.* **269**:960–967.
- Takagi, J., Petre, B., Walz, T., and Springer, T. 2002. Global conformational rearrangements in integrin extracellular domains in outside-in and inside-out signaling. *Cell*. **110**:599–611.
- Lu, C., Takagi, J., and Springer, T.A. 2001. Association of the membrane proximal regions of the  $\alpha$  and  $\beta$  subunit cytoplasmic domains constrains an integrin in the inactive state. *J. Biol. Chem.* **276**:14642–14648.
- Takagi, J., Erickson, H.P., and Springer, T.A. 2001. C-terminal opening mimics 'inside-out' activation of integrin  $\alpha_5\beta_1$ . *Nat. Struct. Biol.* **8**:412–416.
- Kim, M., Carman, C.V., and Springer, T.A. 2003. Bidirectional transmembrane signaling by cytoplasmic domain separation in integrins. *Science*. **301**:1720–1725.
- Adair, B.D., and Yeager, M. 2002. Three-dimensional model of the human platelet integrin  $\alpha_{IIb}\beta_3$  based on electron cryomicroscopy and x-ray crystallography. *Proc. Natl. Acad. Sci. U. S. A.* **99**:14059–14064.
- Xiong, J.P., Stehle, T., Goodman, S.L., and Arnaout, M.A. 2003. New insights into the structural basis of integrin activation. *Blood*. **102**:1155–1159.
- O'Toole, T.E., et al. 1994. Integrin cytoplasmic domains mediate inside-out signal transduction. *J. Cell Biol.* **124**:1047–1059.
- Hughes, P.E., et al. 1996. Breaking the integrin hinge. A defined structural constraint regulates integrin signaling. *J. Biol. Chem.* **271**:6571–6574.
- Chen, Y., et al. 1992. Ser752→Pro mutation in the cytoplasmic domain of integrin  $\beta_3$  subunit and defective activation of platelet integrin  $\alpha_{IIb}\beta_3$  (glycoprotein IIb-IIIa) in a variant of Glanzmann thrombasthenia. *Proc. Natl. Acad. Sci. U. S. A.* **89**:10169–10173.
- Wang, R., Shattil, S.J., Ambruso, D.R., and Newman, P.J. 1997. Truncation of the cytoplasmic domain of  $\beta_3$  in a variant form of Glanzmann thrombasthenia abrogates signaling through the integrin  $\alpha_{IIb}\beta_3$  complex. *J. Clin. Invest.* **100**:2393–2403.
- O'Toole, T.E., Ylanne, J., and Culley, B.M. 1995. Regulation of integrin affinity states through an NPXY motif in the beta subunit cytoplasmic domain. *J. Biol. Chem.* **270**:8553–8558.
- Ylanne, J., et al. 1995. Mutation of the cytoplasmic domain of the integrin beta 3 subunit. Differential effects on cell spreading, recruitment to adhesion plaques, endocytosis, and phagocytosis. *J. Biol. Chem.* **270**:9550–9557.
- Xi, X., Bodnar, R.J., Li, Z., Lam, S.C., and Du, X. 2003. Critical roles for the COOH-terminal NITY and RGT sequences of the integrin beta3 cytoplasmic domain in inside-out and outside-in signaling. *J. Cell Biol.* **162**:329–339.
- Leisner, T.M., Wencel-Drake, J.D., Wang, W., and Lam, S.C.-T. 1999. Bidirectional transmembrane modulation of integrin  $\alpha_{IIb}\beta_3$  conformations. *J. Biol. Chem.* **274**:12945–12949.
- Vinogradova, O., Haas, T., Plow, E.F., and Qin, J. 2000. A structural basis for integrin activation by the cytoplasmic tail of the  $\alpha_{IIb}$  subunit. *Proc. Natl. Acad. Sci. U. S. A.* **97**:1450–1455.
- Haas, T.A., and Plow, E.F. 1996. The cytoplasmic domain of  $\alpha_{IIb}\beta_3$  beta3. A ternary complex of the integrin  $\alpha$  and beta subunits and a divalent cation. *J. Biol. Chem.* **271**:6017–6026.
- Vallar, L., et al. 1999. Divalent cations differentially regulate integrin  $\alpha_{IIb}$  cytoplasmic tail binding to  $\beta_3$  and to calcium- and integrin-binding protein. *J. Biol. Chem.* **274**:17257–17266.
- Weljie, A.M., Hwang, P.M., and Vogel, H.J. 2002. Solution structures of the cytoplasmic tail complex from platelet integrin  $\alpha_{IIb}$  and beta 3-subunits. *Proc. Natl. Acad. Sci. U. S. A.* **99**:5878–5883.
- Vinogradova, O., et al. 2002. A structural mechanism of integrin  $\alpha_{IIb}\beta_3$  "inside-out" activation as regulated by its cytoplasmic face. *Cell*. **110**:587–597.
- Vinogradova, O., et al. 2004. Membrane-mediated structural transitions at the cytoplasmic face during integrin activation. *Proc. Natl. Acad. Sci. U. S. A.* **101**:4094–4099.
- Li, R., et al. 2001. Oligomerization of the integrin  $\alpha_{IIb}\beta_3$ : roles of the transmembrane and cytoplasmic domains. *Proc. Natl. Acad. Sci. U. S. A.* **98**:12462–12467.
- Ulmer, T.S., Yaspan, B., Ginsberg, M.H., and Campbell, I.D. 2001. NMR analysis of structure and dynamics of the cytosolic tails of integrin  $\alpha_{IIb}\beta_3$  in aqueous solution. *Biochemistry*. **40**:7498–7508.
- Naik, U.P., Patel, P.M., and Parise, L.V. 1997. Identification of a novel calcium-binding protein that interacts with the integrin  $\alpha_{IIb}$  cytoplasmic domain. *J. Biol. Chem.* **272**:4651–4654.
- Kato, A., et al. 2002. Ancient ubiquitous protein 1 binds to the conserved membrane-proximal sequence of the cytoplasmic tail of the integrin  $\alpha$  subunits that plays a crucial role in the inside-out signaling of  $\alpha_{IIb}\beta_3$ . *J. Biol. Chem.* **277**:28934–28941.
- Larkin, D., et al. 2004. ICln, a novel integrin  $\alpha_{IIb}\beta_3$ -associated protein, functionally regulates



- platelet activation. *J. Biol. Chem.* **279**:27286–27293.
59. Vijayan, K.V., Liu, Y., Li, T.T., and Bray, P.F. 2004. Protein phosphatase 1 associates with the integrin alphaIIb subunit and regulates signaling. *J. Biol. Chem.* **279**:33039–33042.
60. Armulik, A., Nilsson, I., von Heijne, G., and Johansson, S. 1999. Determination of the border between the transmembrane and cytoplasmic domains of human integrin subunits. *J. Biol. Chem.* **274**:37030–37034.
61. Stefansson, A., Armulik, A., Nilsson, I., von Heijne, G., and Johansson, S. 2004. Determination of N- and C-terminal borders of the transmembrane domain of integrin subunits. *J. Biol. Chem.* **279**:21200–21205.
62. Feral, C.C., et al. 2005. CD98hc (SLC3A2) mediates integrin signaling. *Proc. Natl. Acad. Sci. U. S. A.* **102**:355–360.
63. Buensuceso, C.S., Arias-Salgado, E.G., and Shattil, S.J. 2004. Protein-protein interactions in platelet alphaIIb beta3 signaling. *Semin. Thromb. Hemost.* **30**:427–439.
64. Phillips, D.R., Prasad, K.S., Manganello, J., Bao, M., and Nannizzi-Alaimo, L. 2001. Integrin tyrosine phosphorylation in platelet signaling. *Curr. Opin. Cell Biol.* **13**:546–554.
65. Shattil, S.J., et al. 1995.  $\beta_3$ -Endonexin, a novel polypeptide that interacts specifically with the cytoplasmic tail of the integrin  $\beta_3$  subunit. *J. Cell Biol.* **131**:807–816.
66. Kashiwagi, H., et al. 1997. Affinity modulation of platelet integrin  $\alpha_{IIb}\beta_3$  by  $\beta_3$ -endonexin, a selective binding partner of the  $\beta_3$  integrin cytoplasmic tail. *J. Cell Biol.* **137**:1433–1443.
67. Eigenthaler, M., Hofferer, L., Shattil, S.J., and Ginsberg, M.H. 1997. A conserved sequence motif in the integrin  $\beta_3$  cytoplasmic domain is required for its specific interaction with  $\beta_3$ -endonexin. *J. Biol. Chem.* **272**:7693–7698.
68. Li, R., et al. 2002. Characterization of the monomeric form of the transmembrane and cytoplasmic domains of the integrin beta 3 subunit by NMR spectroscopy. *Biochemistry.* **41**:15618–15624.
69. Calderwood, D.A. 2004. Talin controls integrin activation. *Biochem. Soc. Trans.* **32**:434–437.
70. Calderwood, D.A., et al. 2002. The phosphotyrosine binding (PTB)-like domain of talin activates integrins. *J. Biol. Chem.* **277**:21749–21758.
71. Garcia-Alvarez, B., et al. 2003. Structural determinants of integrin recognition by talin. *Mol. Cell.* **11**:49–58.
72. Ulmer, T.S., Calderwood, D.A., Ginsberg, M.H., and Campbell, I.D. 2003. Domain-specific interactions of talin with the membrane-proximal region of the integrin beta3 subunit. *Biochemistry.* **42**:8307–8312.
73. Patil, S., et al. 1999. Identification of a talin-binding site in the integrin beta(3) subunit distinct from the NPLY regulatory motif of post-ligand binding functions. *J. Biol. Chem.* **274**:28575–28583.
74. Calderwood, D.A., et al. 1999. The talin head domain binds to integrin beta subunit cytoplasmic tails and regulates integrin activation. *J. Biol. Chem.* **274**:28071–28074.
75. Tadokoro, S., et al. 2003. Talin binding to integrin beta tails: a final common step in integrin activation. *Science.* **302**:103–106.
76. Pearson, M.A., Reczek, D., Bretscher, A., and Karplus, P.A. 2000. Structure of the ERM protein moesin reveals the FERM domain fold masked by an extended actin binding tail domain. *Cell.* **101**:259–270.
77. Yan, B., Calderwood, D.A., Yaspan, B., and Ginsberg, M.H. 2001. Calpain cleavage promotes talin binding to the beta 3 integrin cytoplasmic domain. *J. Biol. Chem.* **276**:28164–28170.
78. Fox, J.E., Taylor, R.G., Taffarel, M., Boyles, J.K., and Goll, D.E. 1993. Evidence that activation of platelet calpain is induced as a consequence of binding of adhesive ligand to the integrin, glycoprotein IIb-IIIa. *J. Cell Biol.* **120**:1501–1507.
79. Martel, V., et al. 2001. Conformation, localization, and integrin binding of talin depend on its interaction with phosphoinositides. *J. Biol. Chem.* **276**:21217–21227.
80. Popot, J.L., and Engelman, D.M. 2000. Helical membrane protein folding, stability, and evolution. *Annu. Rev. Biochem.* **69**:881–922.
81. Russ, W.P., and Engelman, D.M. 2000. The GxxxG motif: a framework for transmembrane helix-helix association. *J. Mol. Biol.* **296**:911–919.
82. Senes, A., Gerstein, M., and Engelman, D.M. 2000. Statistical analysis of amino acid patterns in transmembrane helices: the GxxxG motif occurs frequently and in association with beta-branched residues at neighboring positions. *J. Mol. Biol.* **296**:921–936.
83. Dawson, J.P., Melnyk, R.A., Deber, C.M., and Engelman, D.M. 2003. Sequence context strongly modulates association of polar residues in transmembrane helices. *J. Mol. Biol.* **331**:255–262.
84. Schneider, D., and Engelman, D.M. 2004. Involvement of transmembrane domain interactions in signal transduction by alpha/beta integrins. *J. Biol. Chem.* **279**:9840–9846.
85. Li, R., et al. 2003. Activation of integrin alphaIIb beta3 by modulation of transmembrane helix associations. *Science.* **300**:795–798.
86. Li, R., Bennett, J.S., and Degrad, W.F. 2004. Structural basis for integrin alphaIIb beta3 clustering. *Biochem. Soc. Trans.* **32**:412–415.
87. Li, W., et al. 2005. A push-pull mechanism for regulating integrin function. *Proc. Natl. Acad. Sci. U. S. A.* **102**:1424–1429.
88. Fox, J.E., et al. 1996. The platelet cytoskeleton stabilizes the interaction between alphaIIb beta3 and its ligand and induces selective movements of ligand-occupied integrin. *J. Biol. Chem.* **271**:7004–7011.
89. Kim, M., Carman, C.V., Yang, W., Salas, A., and Springer, T.A. 2004. The primacy of affinity over clustering in regulation of adhesiveness of the integrin  $\alpha_4\beta_2$ . *J. Cell Biol.* **167**:1241–1253.
90. Luo, B.H., Carman, C.V., Takagi, J., and Springer, T.A. 2005. Disrupting integrin transmembrane domain heterodimerization increases ligand binding affinity, not valency or clustering. *Proc. Natl. Acad. Sci. U. S. A.* **102**:3679–3684.
91. Luo, B.H., Springer, T.A., and Takagi, J. 2004. A specific interface between integrin transmembrane helices and affinity for ligand. *PLoS Biol.* **2**:e153.
92. Partridge, A.W., Liu, S., Kim, S., Bowie, J.U., and Ginsberg, M.H. 2005. Transmembrane domain helix packing stabilizes integrin alphaIIb beta3 in the low affinity state. *J. Biol. Chem.* **280**:7294–7300.
93. MacKenzie, K.R., Prestegard, J.H., and Engelman, D.M. 1997. A transmembrane helix dimer: structure and implications. *Science.* **276**:131–133.
94. Gottschalk, K.E., Adams, P.D., Brunger, A.T., and Kessler, H. 2002. Transmembrane signal transduction of the alpha(IIb)beta(3) integrin. *Protein Sci.* **11**:1800–1812.
95. Gottschalk, K.E., and Kessler, H. 2004. Evidence for hetero-association of transmembrane helices of integrins. *FEBS Lett.* **557**:253–258.
96. Gottschalk, K.E. 2005. A coiled-coil structure of the alphaIIb beta3 integrin transmembrane and cytoplasmic domains in its resting state. *Structure (Camb.)* **13**:703–712.
97. Arnaout, M.A., Mahalingam, B., and Xiong, J.P. 2005. Integrin structure, allostery, and bidirectional signaling. *Annu. Rev. Cell Dev. Biol.* doi:10.1146/annurev.cellbio.21.090704.151217.
98. Poncz, M., et al. 1987. Structure of the platelet membrane glycoprotein IIb. *J. Biol. Chem.* **262**:8476–8482.
99. Zimrin, A.B., et al. 1988. Structure of platelet glycoprotein IIIa. *J. Clin. Invest.* **81**:1470–1475.